# Optimization of High-Efficiency Organic-Inorganic Lead Halide Perovskite Solar Cells via a Novel Polycaprolactone Additive Pathway

## Introduction

In 2017, natural gas, coal, and oil accounted for nearly 77.6% of U.S. primary energy consumption. Such nonrenewable energy sources are, as the name implies, in limited supply, and according to the U.S. Energy Information Administration, can meet our energy needs for a maximum of 150 years. It is estimated that human activities, primarily our use of energy, account for approximately 35 billion metric tons of carbon dioxide emissions each year, resulting in record high temperatures since the 1980s, a large number of endangered species, and a 160% increase in asthma cases over the past 15 years. Our dependence on nonrenewable energy sources is clearly unsustainable and for this reason, there has been a significant movement towards the use of renewable energy.

Solar power has emerged as one of the most promising sources of renewable energy. Photovoltaic (PV) cells are low maintenance, environmentally friendly devices that convert the energy from sunlight directly into electricity. Currently, there are two major types of PV technologies. The first, wafer-based devices, includes the crystalline silicon cells that are most commonly used in commercial applications. However, due to their high cost, onerous preparation procedures, and limited efficiencies, many are looking to high efficiency thin-film PV cells as a potential replacement in the future. Typically, thin-film solar cells consist of two electrodes, a light-absorbing layer, and various charge transport layers. The absorption of incident photons creates charge carriers (electrons, e-, and holes, h+), which subsequently travel through the electron and hole transport layers (ETLs and HTLs), respectively, and to the electrodes. Much attention has been given to the light-absorbing layer; research groups have studied a multitude of semiconducting materials in an effort to enhance the efficiency of thin-film PV cells.

Perovskite materials are compounds with the same crystalline structure as calcium titanate, $ABX_3$. Their unique properties have led to numerous applications in such devices as light-emitting diodes, lasers, and photodetectors. Additionally, their high absorption coefficient, wide absorption range, stability, tunable band gaps, low exciton binding energy, long carrier diffusion length, high ambipolar charge mobilities, and extended charge carrier lifetime make perovskites one of the best candidates for the light-absorbing layer in next-generation solar cells. In the field of photovoltaics, the most extensively investigated perovskites are organometal trihalides, specifically, methylammonium lead iodide ($CH_3NH_3PbI_3$, or $MAPbI_3$). The structure of $MAPbI_3$ is shown in Figure 1. Group A ($MA^+$) is located at the vertices of the face-centered cubic, the metal cation B ($Pb^{2+}$) resides at the core of the octahedron, the halogen anions X ($I^-$) occupy its apices.

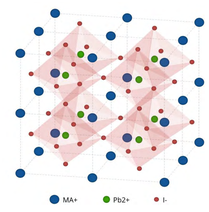


Fig. 1. Crystal structure of $MAPbI_3$ perovskite, which adheres to the general formula $ABX_3$. Group A ($MA^+$, shown in blue) is located at the vertices of the face-centered cubic; the metal cation B ($Pb^{2+}$, shown in green) resides at the core of the octahedron; and the halogen anions X ($I^-$, shown in red) occupy its apices.

## Literature Review

In a just a few years, the performance of perovskite solar cells (PSCs) has exceeded that of dye-sensitized solar cells (DSSCs), organic PV cells, and inorganic nanoparticle-based cells. Initial studies applied perovskites as sensitizers to liquid-electrolyte-based DSSCs, achieving a power conversion efficiency (PCE) of approximately 3%.

3 years later, in 2012, Park et al. raised the PCE to 9.7% by fabricating a solid-state mesoscopic perovskite DSSC. The real breakthrough, however, occurred when Snaith et al. deviated from the DSSC structure and used a mesoporous scaffold to integrate perovskite as the light-absorbing layer, wherein it served as the main source of photogenerated electron-hole pairs. Since then, PSCs have achieved certified PCEs as high as 22.1%, although such efficiencies tend to be very difficult to reliably reproduce.

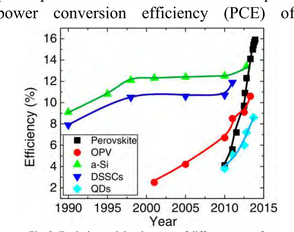


Fig. 2. Evolution and development of different types of thin-film photovoltaic technologies.
*Image taken from Fan et al. "Perovskite-based low-cost and high-efficiency hybrid halide solar cells." Photon. Res. 2, 111-120 (2014).*

Beginning with Snaith et al., the initial evolution of PSCs was based on a mesoscopic metal oxide structure (Figure 2). In such an architecture, the perovskite can be incorporated either as a thin layer to cover the mesoporous metal oxide scaffold or as a layer on top of and infiltrating the scaffold. Historically, these mesoscopic PSCs have performed better than their alternative, the planar heterojunction (PHJ) solar cell. However, the wide variety of both deposition techniques and charge-selective transporting layers compatible with the PHJ structure has made it more realistic moving forward. A conventional n-i-p PHJ PSC consists of a transparent, conductive substrate/n-type ETL/perovskite/p-type HTL/metal electrode. Compact $TiO_2$ (c-$TiO_2$) is the most commonly used ETL; N2,N2,N2′,N2′,N7,N7,N7′,N7′-octakis(4-methoxyphenyl)-9,9′-spirobi[9H-fluorene]-2,2′,7,7′-tetramine (spiro-OMeTAD), the most commonly used HTL. PHJ PSCs have reached efficiencies of up to 20.8%, values comparable to those of their mesoscopic counterparts.

The one-step solution processing technique, a simple and cheap method of fabricating perovskite layers, is one of the most viable ways of scaling PHJ PSCs in the future. However, it often introduces large energy losses during device operation, as the inability to control the crystallization process leads to poor film morphology. A high surface roughness and incomplete coverage, characterized by the presence of point and interstitial defects in the crystal lattice, results in low-resistance shunting paths, insufficient light absorption, and decreased charge separation. Furthermore, grain boundaries (GBs) induce trap states as well as crystal degradation, and exhibit shorter charge carrier lifetime, weaker photoluminescence (PL) intensity, different electrical potentials, and faster ion migration. These properties of GBs lead to nonradiative energy loss, decreased open-circuit voltage, and thus reduced PCE. Recently, several efforts have been made to synthesize perovskite thin films with low surface roughness, complete coverage, ordered crystallites, and fewer grain boundaries via one-step solution processing.

One of these proposed techniques is additive engineering. Previous studies have shown that most successful additives interact with solutes in the perovskite precursor solution (MAI, $PbI_2$), which reduces the speed of crystal formation and provides homogeneous nucleation sites. This results in a controlled arrangement of larger crystals and improved surface morphology. Additionally, nearly all additives have no effect on the tetragonal crystallinity of the perovskite layer; in fact, many studies showed improved crystallinity with the additive.

So far, a few types of additives have been successfully incorporated into PSCs, including chlorides, organics, and organic halide salts. Research on the effects of chloride additives has revealed that while chlorides of all volatilities improve surface morphology, those with low volatility did so without resulting in undesirable byproducts, such as an intermediate phase or a precipitate. This finding may be useful if applied to polymer additives, which have not been widely investigated. One recent study that explored the addition of poly(ethylene glycol) (PEG) reported that the additive retarded aggregation of perovskite crystals and facilitated the production of a smooth layer. This research suggests that polymer additives with low volatility may enhance the PCE of PSCs.

## Engineering Objective

Polycaprolactone (PCL) is an environmentally-friendly aliphatic polyester composed of hexanoate repeat units (Figure 3). Its biodegradability makes it very suitable for use in the biomedical field, including tissue engineering, drug delivery, medical devices, packaging, and composites. Moreover, it is an easily-processable polymer with low volatility that is soluble in polar substances, a rare characteristic of polymers but a necessary one for application to photovoltaic devices. Thus, we expect the addition of PCL in the perovskite layer to enhance the efficiency of planar, thin-film PSCs.

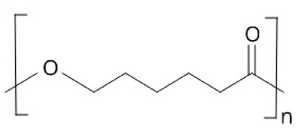


Fig. 3. Chemical structure of polycaprolactone (PCL), a polyester.

The purpose of this study is to investigate the effects of different concentrations of a novel PCL additive on the performance of PSCs and the mechanisms for the enhancement of efficiency, if any. In this paper, we report a simple and original strategy to increase the PCE of perovskite solar cells.

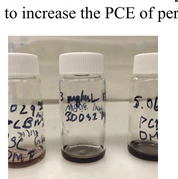

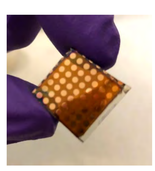

Left: perovskite precursor solution that we prepared in the laboratory.

Right: final PCL-perovskite solar cell we fabricated in the laboratory.

*All graphs and images were student developed unless otherwise cited.*

## Fabrication of Perovskite Solar Cells

To characterize PCL-doped $MAPbI_3$ thin film, glass/c-$TiO_2$/PCL-doped $MAPbI_3$ structures were fabricated (Figure 4) and then analyzed. To measure the performance of PCL-doped $MAPbI_3$ PSCs, full devices were constructed and subsequently analyzed (Figure 5).

- **Synthesis of PCL-Doped $MAPbI_3$ Thin Film**:
  1. Diamond-tip cutters were used to cut microscope slides into square panels of approximately 1.3 cm by 1.3 cm.
  2. The glass samples underwent UV-Ozone treatment for 10 minutes to remove all organic residues.
  3. TiO2 precursor solution was spin-coated onto each glass substrate. The c-$TiO_2$-coated glass was annealed at 465°C for 2 hours and cooled for 30 minutes.
  4. Five perovskite precursor solutions with varying concentrations of PCL (0.0, 0.1, 0.3, 0.6, and 1.0 mg/mL) were prepared.
  5. These precursor solutions were spin-coated onto the c-TiO2 glass (Figure 4).
  6. The films were then annealed at 100°C for 10 minutes.
- **Characterization of PCL-Doped $MAPbI_3$ Thin Film**:
  1. Atomic Force Microscopy (AFM)
  2. Ultraviolet-Visible (UV-Vis) Spectroscopy
  3. Scanning Electron Microscopy (SEM)
  4. X-Ray Diffraction (XRD)
- **Synthesis of PCL-Doped Perovskite Solar Cells:**
  1. $TiO_2$ and PCL-doped $MAPbI_3$ layers were deposited on FTO glass using the procedure described above.
  2. Spiro-OMeTAD solution was prepared and spin-coated onto each panel.
  3. Physical vapor deposition (PVD) was used to add a total of 0.6 g of circular electrodes to the surface of each panel.
  4. The solvent toluene was used to wipe away the perovskite, spiro-OMeTAD, and gold electrodes from the sliver of the panel without $TiO_2$.
  5. Silver paste was dripped onto this portion of the cell.
- **Efficiency of PCL-Doped Perovskite Solar Cells:**
  1. Reverse-scan efficiency test under 1 Sun air mass 1.5 global illumination conditions in ambient air was conducted.

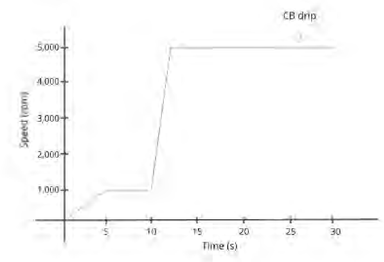


Fig. 4. Speed-time graph of perovskite spin-coating. As part of the solvent engineering technique used, chlorobenzene was dripped onto the spinning cell 3-4 seconds before the spinning finished.

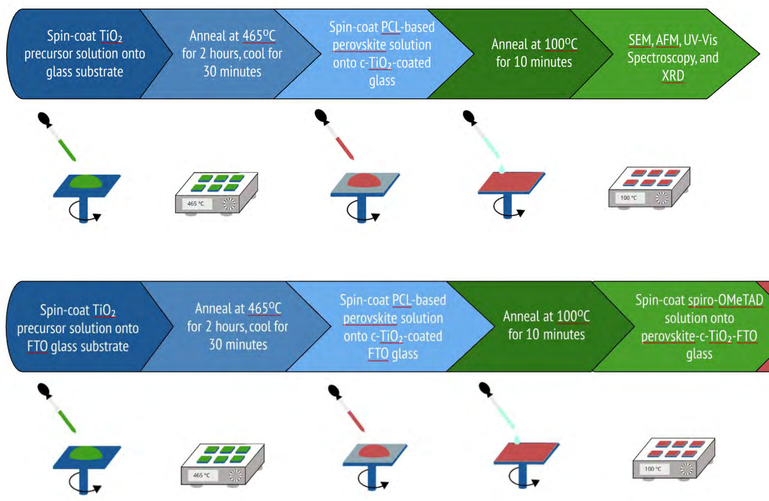


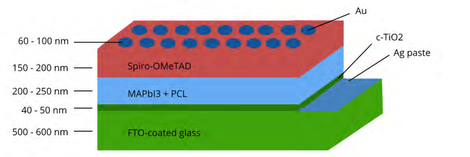


Fig. 5. Device architecture of the perovskite solar cell: FTO glass/$TiO_2$/PCL-doped $MAPbI_3$ perovskite/spiro-OMeTAD/Au, in which $TiO_2$ functions as the electron-transport layer, PCL-doped $MAPbI_3$ as the light-absorbing layer, spiro-OMeTAD as the-transport layer, and gold as an electrode. The silver paste functioned as the other electrode.

## Characterization of Perovskite Thin Film

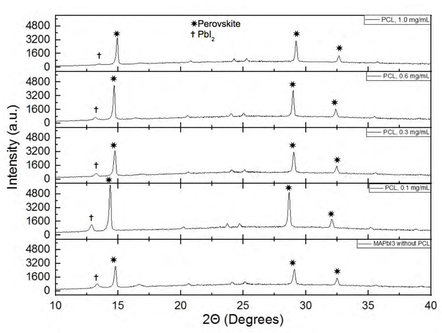


Fig. 6. Diffractograms from XRD analysis of perovskite films with varying amounts of polymer additive. Characteristic perovskite and $PbI_2$ peaks are seen for all samples, but are more intense for samples with 0.1 and 0.6 mg/mL PCL concentrations.

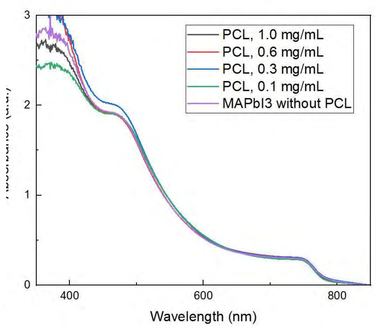


Fig. 7. Complete UV-Vis spectra of perovskite films processed with the varying concentrations of PCL, measured for the range 350-850 nm.

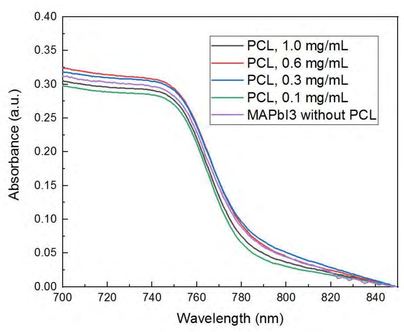


Fig. 8. Absorbance edges for all samples, obtained from the complete UV-Vis spectra of the films.

✓ Comparable X-ray diffraction (XRD) patterns ⊳ unchanged tetragonal crystallinity of $MAPbI_3$

✓ Similar UV-Vis spectral shapes ⊳ optical properties of $MAPbI_3$ layer not compromised

✓ Absorbance values near 750 nm band edge ⊳ similar thicknesses (loading amount unaffected)

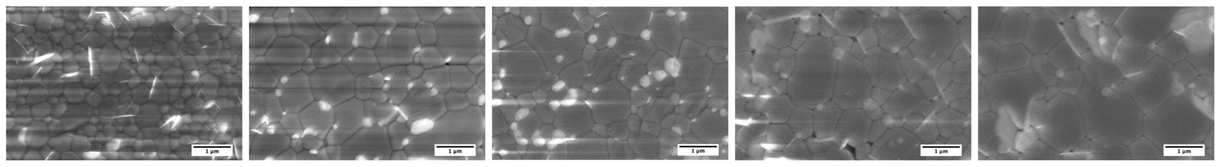

Fig. 9. Planeview SEM images showing the grain sizes of $MAPbI_3$ perovskite films with (a) 0.0, (b) 0.1, (c) 0.3, (d) 0.6, and (e) 1.0 mg/mL PCL additive. All films were obtained by direct one-step spin-coating of the perovskite precursor solution with a simultaneous chlorobenzene drip.

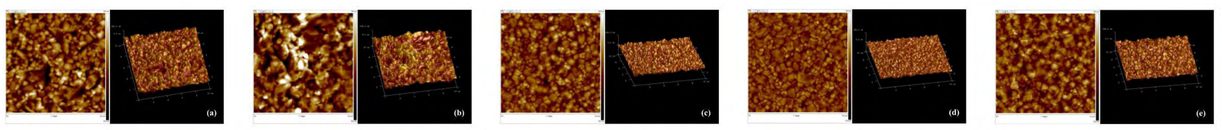


Fig. 10. AFM topography (left) and three-dimensional views (right) of the surface of the $MAPbI_3$ perovskite films with (a) 0.0, (b) 0.1, (c) 0.3, (d) 0.6, and (e) 1.0 mg/mL PCL dopant.

| | Average Particle Size (nm) | Standard Deviation of Particle Size (nm) | RMS (nm) |
|---|---|---|---|
| $MAPbI_3$ without PCL | 376 | 143 | 19.7 |
| PCL, 0.1 mg/mL | 738 | 280 | 19.8 |
| PCL, 0.3 mg/mL | 625 | 289 | 11.2 |
| PCL, 0.6 mg/mL | 672 | 309 | 8.54 |
| PCL, 1.0 mg/mL | 901 | 453 | 11.5 |

Table 1. Summary of parameters for distribution of grain size (nm) obtained from SEM images and root mean square roughness (RMS) values for each film, obtained from AFM analysis. Both average particle size and standard deviation of particle size seem to be positively correlated with PCL concentration.

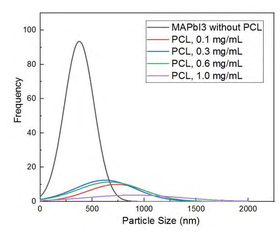


Fig. 11. Distribution of grain size (nm) obtained from SEM images using the ImageJ software.

- Films doped with any concentration of PCL show larger grain size and fewer grain boundaries than their pure counterpart. Because grain boundaries (GBs) have been found to induce trap states, crystal degradation, faster ion migration, and shorter charge carrier lifetimes, devices are expected to exhibit enhanced efficiency.
- The larger grain size can be accounted for by the stronger interactions between the functional groups of PCL and the components of the perovskite precursor solution during spin-coating, which slows the crystallization rate.
- XRD analysis suggests that the bright spots at GBs on SEM images for 0.1 and 0.3 mg/mL PCL are residual $PbI_2$ from the precursor solution. We expected this to enhance efficiency via surface passivation.
- Of the root-mean-square roughness (RMS) values collected from atomic force microscopy (AFM), the 0.6 mg/mL PCL-doped film had the lowest roughness of only 8.54 nm. The low film roughness improves interfacial contact between $MAPbI_3$ and spiro-OMeTAD, resulting in better charge separation and transport.

## Efficiency of Photovoltaic Devices

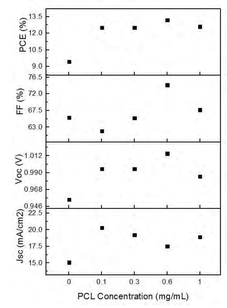


Fig. 12. Scatterplots of short-circuit current density ($J_{SC}$), open-circuit voltage ($V_{OC}$), fill factor (FF), and power conversion efficiency (PCE) for all dopant concentrations.

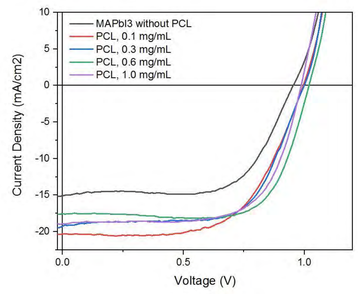


Fig. 13. Current density-voltage (J-V) curves for devices with the different dopant concentrations, measured at reverse scan under air mass 1.5 global (AM1.5G) illumination.

- PCE can increase by up to 39.7% after optimizing the amount of polymer, 0.6 mg/mL.
- Short-circuit photocurrent density (JSC) increased but did not depend on doping concentration.
- Open-circuit voltage ($V_{OC}$) and fill factor (FF) peaked at 0.6 mg/mL.
- Conclusion: these peaks are the result of a balance between two opposing phenomena.
- Larger grain size, fewer GBs, fewer trap centers, and surface passivation that result from the addition of PCL.
- Insulating characteristic of PCL - becomes significant enough to hinder carrier transport at higher concentrations.
- Thus, optimal doping concentration of 0.6 mg/mL yields highest efficiency of 13.2% when these two forces are balanced.

| | $J_{SC}$ (mA/cm²) | $V_{OC}$ (V) | FF (%) | PCE (%) |
|---|---|---|---|---|
| $MAPbI_3$ without PCL | 15.08 | 0.955 | 65.6 | 9.45 |
| PCL, 0.1 mg/mL | 20.29 | 0.995 | 61.9 | 12.5 |
| PCL, 0.3 mg/mL | 19.23 | 0.995 | 65.5 | 12.5 |
| PCL, 0.6 mg/mL | 17.52 | 1.015 | 74.4 | 13.2 |
| PCL, 1.0 mg/mL | 18.91 | 0.985 | 67.7 | 12.5 |

Table 2. Extracted photovoltaic parameters from J-V characterization of the devices with different concentrations of PCL.

## Discussion of Results

Films doped with any concentration of PCL show larger grain size and fewer GBs than their pure counterpart (Figures 9 and 11, Table 1). Further analysis of the SEM images resulting in distributions of grain size and their relevant parameters confirmed these findings. Because GBs have been found to induce trap states, crystal degradation, faster ion migration, and shorter charge carrier lifetimes, devices fabricated with PCL-doped films are expected to perform better than those with pure perovskite films.

We speculate that the larger grain size can be accounted for by the stronger interactions between the functional groups of PCL and the components of the perovskite precursor solution during spin-coating. Specifically, the polymer functions as a heterogeneous nucleus in the nucleation step, which reduces interfacial energy. This retards the growth and aggregation of perovskite crystals, thus slowing the crystallization rate and producing larger grains. However, the positive correlation between standard deviation of grain size distribution and PCL concentration indicates that the additive may inhibit homogeneous nucleation during the crystallization process, resulting in a less uniform film. Regardless, large grain size seems to be critical to the function of the PV cell, and we therefore conclude that PCL is beneficial to the perovskite crystallization process.

SEM images reveal several bright spots at GBs, particularly on the films doped with 0.1 and 0.3 mg/mL PCL (Figure 9). Previous studies have shown that these white phases are residual $PbI_2$ from the perovskite precursor solution. XRD analysis shows higher intensity $PbI_2$ peaks for 0.1 and 0.3 mg/mL PCL-doped films, which verifies that this secondary phase at GBs is $PbI_2$ (Figure 6). This is an additional benefit of PCL doping, as previous incorporation of $PbI_2$ into GBs of perovskite films has resulted in higher PCEs.

The intense peaks at 14.70°, 29.00°, and 32.41° in the diffractograms can be respectively assigned to (110), (220), and (310) diffractions of the tetragonal $MAPbI_3$ phase. The comparable XRD patterns exhibited by all films fabricated imply the unchanged tetragonal crystallinity and nearly complete conversion to $MAPbI_3$ perovskite. Furthermore, the increase in intensity of the 14.7° and 29° peaks for films doped with PCL signifies their enhanced crystallinity.

UV-Vis spectrometry was employed to further characterize the perovskite films. As seen in Figure 7, the absorption spectra scanning from ultraviolet to near infrared wavelengths exhibit two distinct shoulders located at ~480 nm and ~750 nm. The comparable spectral shapes demonstrate that the optical properties of the MAPbI3 layer were not compromised by the addition of PCL. Moreover, the similar absorbance values near the 750 nm band edge indicate that the film thickness is almost the same, and therefore the additive did not affect the loading amount of perovskite on the substrate during spin-coating (Figure 8). Because the spectral shapes and XRD peak positions of the films with and without the PCL additive remain unchanged, we propose that the PCL localizes either on the surface of the perovskite film or at its GBs. Additionally, this provides a possible explanation for the presence of $PbI_2$ at the GBs in the SEM images. We hypothesize that when the polymer additive moves to the GBs and the surface during the crystallization process, some $PbI_2$ migrates with it.

We speculate that the presence of $PbI_2$ and PCL at the GBs and surface enhances the efficiency of the fabricated devices via a surface passivation mechanism. Localization of trap-states at the surface and GBs of the perovskite film induces monomolecular recombination, contributing to significant energy loss. The long-chain PCL polymer serves as an efficient passivating agent in the perovskite film due to the formation of weak coordination bonds at the GBs between $Pb^{2+}$ and the oxygen in the ester group of PCL. Thus, it can be reasonably concluded that the addition of PCL ultimately results in suppressed charge recombination and extended carrier diffusion length through surface passivation.

The SEM images revealed the ability of PCL to retard the growth and aggregation of perovskite crystals, and thus it is reasonable to speculate that the additive reduces the surface roughness also. To investigate this theory, AFM images and corresponding root-mean-square roughness (RMS) values were collected and are shown in Figure 10 and Table 1. While all RMS values are relatively low, the perovskite film doped with 0.6 mg/mL PCL has a remarkably low roughness of only 8.54 nm. The low film roughness has the advantage of improving the interfacial contact between the perovskite film and the spiro-OMeTAD layer, resulting in better charge separation and transport. It should be noted, however, that a considerable amount of time passed (3 days) between the fabrication and AFM measurement for the pure perovskite and 0.1 mg/mL PCL-doped films, allowing for significant degradation to occur. This may explain the higher RMS values exhibited by these two films.

J-V curves of the devices are shown in Figure 13, and their performance parameters are summarized in Table 2. The PCE of the PHJ device can achieve up to a 39.7% increase in efficiency after optimizing the amount of polymer. The device fabricated with pure perovskite exhibited a short-circuit photocurrent density ($J_{SC}$) of 15.08 mA/cm2, an open-circuit voltage ($V_{OC}$) of 0.955 V, a fill factor (FF) of 65.6%, and a PCE of 9.45%. When the perovskite contained 0.6 mg/mL PCL, the device showed the most significant improvement with a $J_{SC}$ of 17.52 mA/cm2, $V_{OC}$ of 1.015 V, FF of 74.4%, and high PCE of 13.2%. The stacked graphs (Figure 12) more clearly show the trends in photovoltaic performance parameters for cells doped with different concentrations of PCL.

The value of $J_{SC}$ apparently increased after doping; however, it did not significantly depend on the dopant concentration. We attribute this to the high surface coverage, continuity, and defect passivation of these films. Both $V_{OC}$ and FF show peaks at 0.6 mg/mL and then fall at a higher concentration of PCL. These two factors are the greatest contributors to the highest PCE of 13.2% at 0.6 mg/mL PCL. We propose that these peaks are the result of a balance between two opposing phenomena. The first is the larger grain size, fewer GBs, fewer trap centers, and surface passivation that result from the addition of PCL. These characteristics initially increase the $V_{OC}$, FF, and therefore PCE of devices with the additive. Countering this effect, however, is the insulating characteristic of PCL. At higher concentrations, this property becomes significant enough to hinder carrier transport, causing the accumulation and recombination of charges in the perovskite layer. This has a detrimental effect on device performance, and thus we see that the optimal concentration of PCL, 0.6 mg/mL, yields the highest efficiency of 13.2%.

## Conclusion

We have successfully increased the PCE of the PHJ PSC from 9.45% to 13.2% by adding 0.6 mg/mL PCL to the perovskite film. This additive can improve the morphology of the perovskite layer by controlling the crystallization process, resulting in increased grain size, full coverage, and lower surface roughness. Additionally, PCL and $PbI_2$ at GBs and on the surface function to passivate defect trap-states, further enhancing the performance of the device. The high-efficiency devices fabricated with the novel, biodegradable, and easily-processable PCL dopant suggests its viability as a promising component of future, high-efficiency PSCs.

## Future Research

In the future, the long-term stability of these devices may be improved by applying thin-film encapsulation (TFE) techniques, and may be measured using time-resolved photoluminescence spectroscopy (TRPL). The efficiency of PCL-doped $MAPbI_3$ PSCs may be further increased by engineering the interfaces to facilitate carrier injection into transport layers and extraction at the electrodes.